ACS Energy Letters

http://pubs.acs.org/journal/aelccp

A Fluorinated Alkoxyaluminate Electrolyte for Magnesium-Ion Batteries

Jake T. Herb,[†,‡] Carl A. Nist-Lund,[‡] and Craig B. Arnold*[,‡,§]

[†]Department of Chemistry, [‡]Princeton Institute for the Science and Technology of Materials, and [§]Department of Mechanical and Aerospace Engineering, Princeton University, Princeton, New Jersey 08544, United States

Supporting Information

ABSTRACT: The lack of electrolytes that simultaneously possess high Coulombic efficiency, conductivity, and voltage stability has hindered the deployment of rechargeable magnesium-ion batteries. With few exceptions, the tenacious oxide layer on magnesium metal has limited the scope of research to halide ion-based electrolytes, which help activate the electrode surface but also limit the working voltage window considerably. Herein, we demonstrate a new class of magnesium electrolytes based on fluoroalkoxyaluminate anions synthesized via a facile and scalable method and its incorporation in a full battery cell. Mixtures of magnesium and aluminum fluoroalkoxides in ethereal solvents result in solutions that can reversibly deposit magnesium metal with near unit efficiency in addition to achieving suitable oxidative stabilities (>3.5 V vs Mg/Mg^{2+} on glassy carbon and gold) and conductivities (>6 mS cm^{-1}).

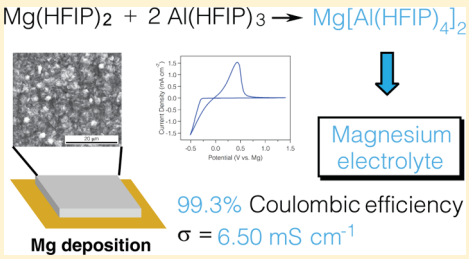

Successful implementation of intermittent energy sources such as wind farms and solar fields is codependent on progress in reliable energy storage, e.g., batteries. Rechargeable battery chemistries that utilize abundant and energy-dense materials such as alkaline earth metals are an attractive choice. Magnesium has been the subject of considerable research because of its high volumetric energy density of 3832 mAh cm^{-3}.[1−3] In this case, the charging and discharging processes consist of electrodepositing and removing magnesium from the anode surface, respectively. Proof of principle for operation of Mg-ion batteries was demonstrated by researchers as early as 1990, but these systems suffered from a number of key limitations in their figures of merit including low conductivity, voltage limits, and Coulombic efficiency due to the composition of the alkyl- or aryl-containing electrolytes.[4−7] Other solutions use non-nucleophilic amides[2,5] or alkoxides[8,9] coupled with $AlCl_3$ to result in electrolytes with more favorable characteristics and greater compatibility with prototype cathode materials, but they still contain halide ions that limit the utility of such formulations in stainless steel coin cells.[10]

As such, it is imperative to develop alternative electrolyte chemistries without in turn sacrificing Coulombic efficiency and conductivity. To date, the only "simple" and commercially available salts capable of reversible Mg electrodeposition have been magnesium bis(trifluoromethylsulfonyl)amide[11] ($Mg(TFSI)_2$) and magnesium borohydride ($Mg(BH_4)_2$).[12,13] Despite moderate improvements to electrolyte performance using glymes[11] or ionic liquids[14] as solvents, the overall performance is not sufficient for practical battery systems. Other previously reported work has shown that bulky, noncoordinating type anions can be used to impart favorable electrochemical characteristics on magnesium electrolyte solutions.[15] Carborane structures such as $Mg(CB_{11}H_{12})_2$ in higher-order glymes have emerged as promising candidates for magnesium electrolytes because of their high oxidative stability, although they result in less than unit Coulombic efficiency in addition to being expensive and nontrivial to synthesize.[3,13,15] More recently, the synthesis and electrochemical activity of $Mg(PF_6)_2$, a compound previously thought to be incapable of reversible Mg deposition, was demonstrated with favorable performance characteristics.[16]

Herein, we report on the development of fluoroalkoxyaluminate-based electrolytes for use in Mg-ion battery systems. Lithium electrolytes incorporating these anions have been previously reported and are known for their high conductivity and electrochemical stability.[17−19] Compounds such as lithium aluminum hexafluoroisopropoxide ($LiAl(HFIP)_4$) are generally synthesized via reaction of $LiAlH_4$ with HFIP.[18] We were motivated to utilize another synthetic route to bypass the need to use a lithium compound followed by a salt metathesis reaction to generate the magnesium salt. Instead, by using a magnesium fluoroalkoxide as a starting material in combination with a Lewis acidic aluminum alkoxide,[9,20−23] we generate an electrolyte that is capable of reversible Mg electrodeposition. Importantly, the magnesium fluoroalkoxyaluminate solution is an easily synthesized, high conductivity electrolyte and is

Received: August 14, 2016
Accepted: November 14, 2016

 © XXXX American Chemical Society

DOI: 10.1021/acsenergylett.6b00356
ACS Energy Lett. 2016, 1, 1227−1232

compatible with prototype cathode materials in full cell battery tests.

The first goal of this work is to illustrate that strongly Lewis acidic aluminum fluoroalkoxides can abstract alkoxide ligands from magnesium fluoroalkoxides to form weakly coordinating aluminate anions in solution (eqs 1−3). This hypothesis is most readily probed using ^{27}Al NMR because of its high sensitivity to changes in coordination.[24] The ^{27}Al NMR spectrum of aluminum hexafluoroisopropoxide ($Al(HFIP)_3$, **1**) in DME exhibits two broad resonances ca. 7.34 ppm ($\nu_{1/2}$ = 820 Hz) and 37.57 ppm ($\nu_{1/2}$ = 1132 Hz), as well as a sharp peak at 61.18 ppm ($\nu_{1/2}$ = 98 Hz) (Figure 1a). The two broad

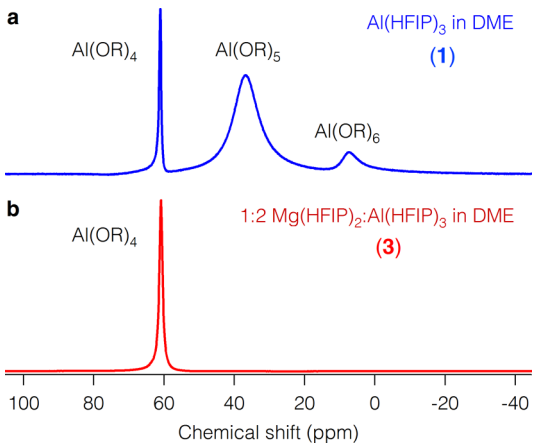

Figure 1. ^{27}Al NMR spectra of electrolyte components in DME: (a) spectrum of $Al(HFIP)_3$ precursor 1 and (b) spectrum of 3, a 1:2 mixture of $Mg(HFIP)_2$:$Al(HFIP)_3$.

resonances have previously been assigned to six-coordinate (7.30 ppm) and five-coordinate (37.57 ppm) aluminum centers present in the tetrameric and trimeric (or solvated) forms of $Al(OR)_3$ species, respectively.[24] The sharp resonance (61.18 ppm) is the result of a symmetric and tetrahedral solution species and is therefore attributed to the four-coordinate aluminum centers in the tetramer.[24] After **1** reacts with magnesium hexafluoroisopropoxide ($Mg(HFIP)_2$, **2**) in DME, the solution of 1:2 $Mg(HFIP)_2$:$Al(HFIP)_3$ (**3**) shows only a sharp resonance at 60.87 ppm ($\nu_{1/2}$ = 142 Hz) in the range of four-coordinate aluminum (Figure 1b). On the basis of this observation, as well as data previously reported for the lithium analogue (^{27}Al δ = 60.55 ppm for $LiAl(HFIP)_4$),[18,21] the primary sharp signal can be attributed to the presence of the tetrahedral $[Al(HFIP)_4]^-$ anion. As such, the proposed structure of the electrolyte solution in this molar ratio is $Mg[Al(HFIP)_4]_2$. The same structure has also been observed in the case of $Mg[Al(OPh)_4]_2$ via combination of the constituent alkoxides,[25] as well as $Mg[Al(OiPr)_4]_2$.[26] In total, these data show that Lewis acidic aluminum alkoxides induce formation of tetrahedrally coordinated aluminate anions.

$$Al(CH_3)_3 + 3HFIP \xrightarrow[0°C,24h]{DME} \underset{(1)}{Al(HFIP)_3} + 3CH_4 \quad (1)$$

$$Mg(OCH_3)_2 + 2HFIP \xrightarrow[RT,24h]{THF} \underset{(2)}{Mg(HFIP)_2} + 2CH_3OH \quad (2)$$

$$\underset{(2)}{Mg(HFIP)_2} + 2\underset{(1)}{Al(HFIP)_3} \xrightarrow[RT,96h]{DME} \underset{(3)}{Mg[Al(HFIP)_4]_2} \quad (3)$$

A few key observations are of note regarding other relevant NMR-active nuclei. ^{25}Mg NMR analysis of solutions of **3** shows shifts within the range of cationic magnesium species (Figure S9), which are in agreement with those of previously reported electrolyte solutions.[27,28] In the case of the system presented here, the diverse set of components and oligomers in each solution makes ^{19}F and ^{1}H spectral deconvolution a challenge. ^{19}F NMR analyses of **1** and **3** exhibit doublets in a narrow range near −77 ppm, with each doublet possessing a $^{3}J_{HF}$ coupling constant (6 Hz) characteristic of the CF_3 group coupling with the proton located on the central carbon (Figures S1 and S7). The presence of multiple doublets is attributed to fluorine's intrinsic sensitivity and coordination of the fluoroalkoxide ligands to metal cations, thereby resulting in slight changes in the magnetic environment of the CF_3 groups.[29,30] Resonances associated with DME in the ^{1}H NMR spectra of the fluoroalkoxide precursors as well as the electrolytes (Figures S3, S6, and S10) are shifted downfield relative to their nonmetalated counterpart because of the electron-withdrawing effect of the metal cations in solution, as has been observed in electrolyte solutions of $Mg(BH_4)_2$ in DME.[13,31] In the synthesis of the precursor **1**, ^{1}H NMR analysis indicates complete conversion to the alkoxide product due to the absence of peaks corresponding to the trimethylaluminum starting material (Figure S3).

While the NMR spectra establish the presence of the fluoroalkoxyaluminate anion, ultimately the electrochemical properties of the solution dictate the viability of an electrolyte. The initial conductivity value of a 0.25 M solution of **2** is 0.50 mS cm^{-1}, and the value is 1.31 mS cm^{-1} for a 0.5 M solution of **1** in DME. After the reaction, a 0.25 M solution of **3** in DME displays a conductivity value of 6.50 mS cm^{-1} at 25 °C, further validating the hypothesis that heterobimetallic alkoxides can be formed by mixing the constituent alkoxides in polar aprotic solvents.[20,21] Furthermore, this value is higher than that of many other simple magnesium salt formulations,[11,14] though it does not reach as high as 0.71 M $Mg(PF_6)_2$ in 1:1 THF:CH_3CN because of the higher dielectric constant of CH_3CN.[16]

The deposition overpotential and Coulombic efficiency of magnesium plating are critical factors for characterizing electrolytes in secondary magnesium-ion cells. The plating overpotential for the first cycle of a 0.25 M solution of **3** in DME is −0.8 V, but the value reduces significantly to −0.35 V after two more cycles (Figure S14). No evidence of Mg passivation was observed over hundreds of plating and stripping cycles (Figure 2a). The initial overpotential for plating can be attributed to the resistive oxide layer on the surface of the magnesium anode, which is removed through successive cycling of the cell. Initial Coulombic efficiency values start ca. 58% but increase to 99.3% with repeated cycling in galvanostatic switching experiments (Figure 2b). This phenomenon is due likely in part to both "electrolyte conditioning" and further breakdown of the passivating layer on the magnesium anode surface.[32] Electrolyte solutions prepared in G2 exhibit a lower plating overpotential (−0.17 V), though this improvement comes at the expense of Coulombic efficiency (43% after 50 cycles) (Figure S15). These data suggest that minute changes in solvent environment can considerably improve electrochemical characteristics, as has been established with other reported Mg-ion electrolytes.[11,13] Mg deposits from $Mg[Al(HFIP)_4]_2$ in DME are dendrite-free, with morphological characteristics similar to that of reported magnesium electrodepositions at

DOI: 10.1021/acsenergylett.6b00356
ACS Energy Lett. 2016, 1, 1227−1232

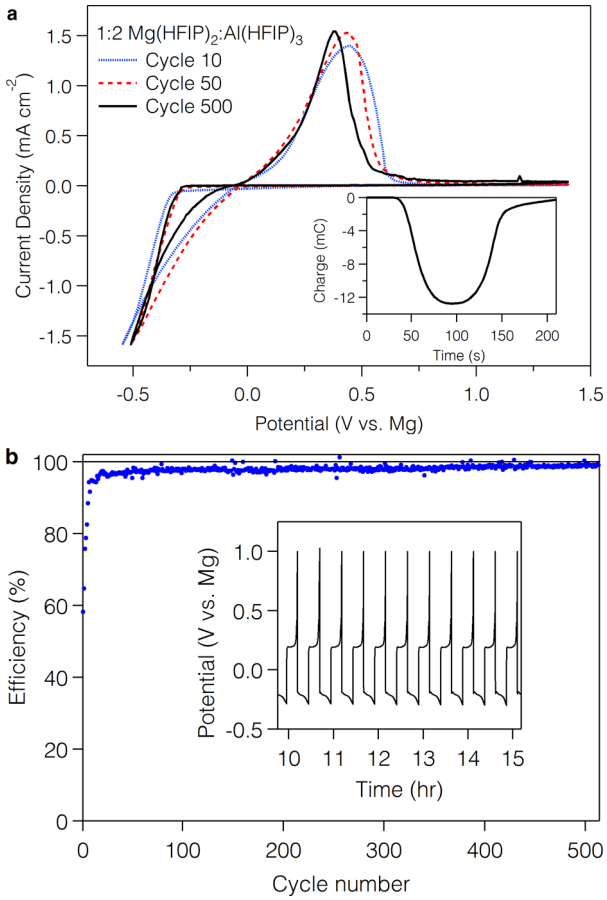

Figure 2. (a) Extended cycling behavior of 0.25 M 3 in DME (scan rate = 10 mV s^{-1}). Inset shows charge passed during cycle 500. (b) Coulombic efficiency as a function of cycle count from a galvanostatic plating and stripping experiment. Inset shows voltage behavior during cycling.

comparable current densities,[28,33] and energy-dispersive X-ray and X-ray photoelectron spectroscopy (XPS) analyses of the deposits indicate the presence of pure Mg (Figure S20).

Because the fluoroalkoxyaluminate anion contains highly electron-withdrawing groups and possesses steric bulk, a high anodic stability is expected. Indeed, the stability of the corresponding lithium compound $LiAl(HFIP)_4$ in DME has previously been reported as >4.6 V vs Li/Li^+ on glassy carbon, limited by solvent oxidation.[19,34] Importantly, onset of anodic current for **3** in DME on both gold and glassy carbon (GC) electrodes begins near 3.5 V vs Mg/Mg^{2+}, though this value is also limited by the oxidation threshold of the solvent (Figure 3).[35] The observed disparity between the Au, GC, and Pt electrodes is likely due to surface-dependent platinum-catalyzed oxidation of a trace amount of protonated HFIP that was not completely removed under vacuum, oxidation of the HFIP ligand via β-hydride elimination, or other decomposition pathways reported previously.[17] To our knowledge, no other data exists for the oxidative behavior of this anion on Pt. Electrolysis of the electrolyte at 3.25 V vs Mg/Mg^{2+} on Pt for 64 h until the current decays to ca. 0 A does not cause significant changes according to NMR other than a small upfield shift of peaks in the ^{19}F, ^{1}H, and ^{25}Mg spectra, likely as a result of a decrease in concentration of Mg^{2+} (Figure S13). Linear sweep voltammetry (LSV) using fresh electrodes shows a substantial decrease in current flow compared to the initial

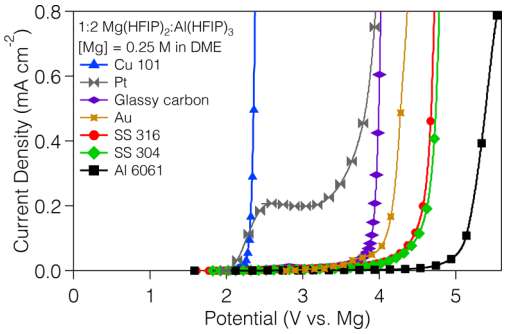

Figure 3. Linear sweep voltammograms of 0.25 M $Mg[Al(HFIP)_4]_2$ (5 mV s^{-1} scan rate) in DME on various electrode substrates.

scan (Figure S17). Use of the Pt-electrolyzed solution also does not have any observable effect on long-term Mg plating and stripping over 800 CV cycles (Figure S16). We hypothesize that the replacement of HFIP with a ligand that does not contain a beta proton or the removal of trace amounts of the reactant from the precursors may inhibit this reactivity that is observed solely on Pt, and this will be the subject of further investigation. LSV data for copper indicate that anodic dissolution of this commonly used current collector occurs at fairly low potentials, precluding its use with high-voltage materials. The apparent high stability on industrially relevant electrodes such as SS and Al, while not representative of the thermodynamic stability of the electrolyte itself, indicates that a surface passivation process is occurring, as is the case for electrolytes that incorporate $Mg(TFSI)_2$ and $Mg(PF_6)_2$.[11,16]

While LSV allows for rapid testing of oxidative stabilities at sufficiently slow scan rates on inert electrodes such as GC and Au, they do not offer a complete picture of the stability of a given electrolyte when paired with practical electrode materials such as Al, SS, or Cu. These materials were investigated further by chronoamperometry to preliminarily determine the nature of any passivation layers or corrosion processes resulting from 2 days of electrolysis at high voltages. For high-purity Al, no changes could be observed by visual inspection, but minor pitting was observed at 3 V, and a greater amount was seen at 3.5 V vs Mg/Mg^{2+} by scanning electron microscopy (SEM) (Figures S21e,S22a). Depth profile XPS data indicate that the oxidized substrates contain an inorganic fluoride surface layer, similar to the oxidation of the PF_6^- anion on Al in lithium-ion electrolytes (Figures S21g and S22f).[36] These aluminum fluoride films are generally viewed as beneficial for their ability to inhibit rapid breakdown of the current collector. Standard aluminum foil, which contains copper, iron, and silicon according to EDS, does not appear to suffer from the same degree of pitting, particularly at 3 V (Figure S24). Corrosion at 3.5 V is concentrated in areas rich in iron intermetallic inclusions, illustrating that small variations in the surface composition can significantly influence the rate and mechanism of metal dissolution (Figure S25). Previous chronoamperometric experiments from the literature concerning oxidative behavior of electrolytes using the $[Al(HFIP)_4]^-$ anion on Al had been performed for only 1 h and did not include SEM or XPS analysis.[19] SS 304 substrates held at 3 and 4 V show similar trends in amounts of pitting by SEM (Figures S27 and S28), while Cu held at 1.9 V shows no sign of corrosion (Figure S30). The data shown here indicate that while this HFIP-based anion or its equilibrium species may undergo or cause surface-dependent oxidative processes at high voltages over longer time

DOI: 10.1021/acsenergylett.6b00356
ACS Energy Lett. 2016, 1, 1227−1232

scales, it is possible that these issues can be ameliorated by incorporating a polyfluorinated ligand lacking a beta proton.[19]

Having synthesized an electrolyte capable of reversible Mg deposition with a suitably large electrochemical window on industrially relevant current collectors, we tested **3** in full battery cells using two prototype cathode materials: Chevrel phase Mo_6S_8 and potassium-stabilized α-MnO_2. Behavior from the first 50 charge−discharge cycles for Mo_6S_8 using **3** in DME (Figure 4) and XRD patterns of the pristine and discharged

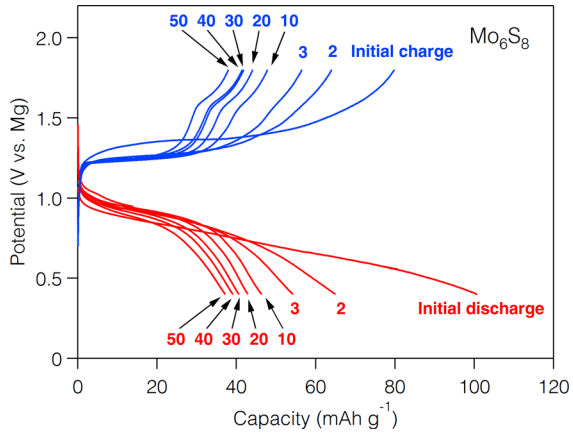

Figure 4. Charge−discharge behavior of Mo_6S_8 cycled at a rate of 10 mA g^{-1} using a 0.25 M solution of 3 in DME. Note that the first cycle begins with a discharge step.

cathode (Figure S18) indicate that intercalation of Mg^{2+} occurs using this electrolyte, though with large overpotentials. This phenomenon is likely due in part to both the cation desolvation−solvation energy and the structure of the electrolyte−cathode interface during the magnesiation and demagnesiation steps; previous reports have shown how both the choice of solvent[41] and anion identity (particularly the presence of chloride ions)[42] have a significant impact on the mechanism and resulting kinetics of this process. This may also explain the capacity loss over the first 50 cycles. The observation of a single voltage plateau upon charge and discharge is similar to that reported for the $Mg(BH_4)_2$ and $Mg(CB_{11}H_{12})_2$ electrolytes.[13,15] While further optimization of the solvent system and fluoroalkoxide ligand will likely improve performance in this respect, the data presented here validate that solutions of **3** can intercalate magnesium ions into Mo_6S_8.

Although α-MnO_2 exhibits a large capacity fade after a minimal number of cycles, it serves as an example of a prototype high-voltage Mg-ion cathode material.[37] The data shown in Figure S19a illustrate charge−discharge behavior characteristic of this material reported previously.[15,38,39] To demonstrate reversible interaction of Mg with the α-MnO_2, XPS spectra from the Mn 3s region from a pristine, discharged, and charged cell are shown in Figure S19b. The difference in binding energy (ΔE_{3s}) between the primary and higher BE satellite peak in this region is inversely related to the average Mn oxidation state.[40] As such, the increase in ΔE_{3s} upon discharging correlates with reduction of the Mn, and vice versa for the charge step. The incomplete reoxidation of Mn is in agreement with previous work detailing the irreversible surface phase transformation that occurs upon discharging this material.[37] Although these results do not show that this combination would make a practical Mg-ion battery, they do demonstrate reversible interaction of Mg^{2+} with this material.

Here, we have demonstrated a new class of electrolytes for magnesium-ion battery systems based on the weakly coordinating anion $[Al(HFIP)_4]^-$ that exhibits high conductivity and reversibly plates Mg with high efficiencies, as well as the use of this solution in full battery cells using prototype cathode materials. The practical oxidative stability of the electrolyte was probed using chronoamperometric methods on Al electrodes, indicating that anodic dissolution may be inhibited, but is not stopped, by formation of an aluminum fluoride layer. Exploration of this class of anions is an important step forward not only in Mg-ion battery chemistry but also for other multivalent ionic systems such as calcium and aluminum. These types of compounds will enable further research on the mechanism of magnesium electrodeposition and can also be easily incorporated into ionic liquid systems. The synthetic ease and customizability of this electrolyte will enable more rapid advancements leading toward commercialization of multivalent secondary batteries.

■ ASSOCIATED CONTENT

Supporting Information

The Supporting Information is available free of charge on the ACS Publications website at DOI: 10.1021/acsenergylett.6b00356.

Experimental details, NMR spectra, and Figures S1−S31 (PDF)

■ AUTHOR INFORMATION

Corresponding Author

*E-mail: cbarnold@princeton.edu.

Notes

The authors declare no competing financial interest.

■ ACKNOWLEDGMENTS

The authors acknowledge funding from Addy/ISN North American Low Carbon Emission Energy Self-Sufficiency Fund at Princeton University, NSF-DGE 1148900, and the PRISM Imaging and Analysis Center, with funding from NSF-DMR 1420541. The authors acknowledge assistance from István Pelczer and Kenith Conover in the Princeton University Department of Chemistry NMR facility. The authors acknowledge Elizabeth Seibel and Kristen Baroudi of the Cava Lab at Princeton University for their assistance in the preparation and characterization of Mo_6S_8.

■ REFERENCES

(1) Muldoon, J.; Bucur, C. B.; Oliver, A. G.; Sugimoto, T.; Matsui, M.; Kim, H. S.; Allred, G. D.; Zajicek, J.; Kotani, Y. Electrolyte Roadblocks to a Magnesium Rechargeable Battery. *Energy Environ. Sci.* **2012**, *5*, 5941−5950.

(2) Kim, H. S.; Arthur, T. S.; Allred, G. D.; Zajicek, J.; Newman, J. G.; Rodnyansky, A. E.; Oliver, A. G.; Boggess, W. C.; Muldoon, J. Structure and Compatibility of a Magnesium Electrolyte with a Sulphur Cathode. *Nat. Commun.* **2011**, *2*, 427−432.

(3) Carter, T. J.; Mohtadi, R.; Arthur, T. S.; Mizuno, F.; Zhang, R.; Shirai, S.; Kampf, J. W. Boron Clusters as Highly Stable Magnesium-Battery Electrolytes. *Angew. Chem., Int. Ed.* **2014**, *53*, 3173−3177.

(4) Aurbach, D.; Lu, Z.; Schechter, A.; Gofer, Y.; Gizbar, H.; Turgeman, R.; Cohen, Y.; Moshkovich, M.; Levi, E. Prototype Systems for Rechargeable Magnesium Batteries. *Nature* **2000**, *407*, 724−727.

(5) Gregory, T. D.; Hoffman, R. J.; Winterton, R. C. Nonaqueous Electrochemistry of Magnesium. *J. Electrochem. Soc.* **1990**, *137*, 775−780.

DOI: 10.1021/acsenergylett.6b00356
ACS Energy Lett. 2016, 1, 1227−1232

(6) Gofer, Y.; Chusid, O.; Gizbar, H.; Viestfrid, Y.; Gottlieb, H. E.; Marks, V.; Aurbach, D. Improved Electrolyte Solutions for Rechargeable Magnesium Batteries. *Electrochem. Solid-State Lett.* **2006**, *9*, A257−A260.
(7) Aurbach, D.; Weissman, I.; Gofer, Y.; Levi, E. Nonaqueous Magnesium Electrochemistry and Its Application in Secondary Batteries. *Chem. Rec.* **2003**, *3*, 61−73.
(8) Liao, C.; Guo, B.; Jiang, D.; Custelcean, R.; Mahurin, S. M.; Sun, X.-G.; Dai, S. Highly Soluble Alkoxide Magnesium Salts for Rechargeable Magnesium Batteries. *J. Mater. Chem. A* **2014**, *2*, 581−584.
(9) Herb, J. T.; Nist-Lund, C.; Schwartz, J.; Arnold, C. B. Structural Effects of Magnesium Dialkoxides as Precursors for Magnesium-Ion Electrolytes. *ECS Electrochem. Lett.* **2015**, *4*, A49−A52.
(10) Muldoon, J.; Bucur, C. B.; Oliver, A. G.; Zajicek, J.; Allred, G. D.; Boggess, W. C. Corrosion of Magnesium Electrolytes: Chlorides − the Culprit. *Energy Environ. Sci.* **2013**, *6*, 482−487.
(11) Ha, S. Y.; Lee, Y. W.; Woo, S. W.; Koo, B.; Kim, J. S.; Cho, J.; Lee, K. T.; Choi, N. S. Magnesium(II) Bis(trifluoromethane Sulfonyl) Imide-Based Electrolytes with Wide Electrochemical Windows for Rechargeable Magnesium Batteries. *ACS Appl. Mater. Interfaces* **2014**, *6*, 4063−4073.
(12) Tutusaus, O.; Mohtadi, R. Paving the Way towards Highly Stable and Practical Electrolytes for Rechargeable Magnesium Batteries. *ChemElectroChem* **2015**, *2*, 51−57.
(13) Mohtadi, R.; Matsui, M.; Arthur, T. S.; Hwang, S. Magnesium Borohydride: From Hydrogen Storage to Magnesium Battery. *Angew. Chem., Int. Ed.* **2012**, *51*, 9780−9783.
(14) Watkins, T.; Kumar, A.; Buttry, D. A. Designer Ionic Liquids for Reversible Electrochemical Deposition/ Dissolution of Mg. *J. Am. Chem. Soc.* **2016**, *138*, 641−650.
(15) Tutusaus, O.; Mohtadi, R.; Arthur, T. S.; Mizuno, F.; Nelson, E. G.; Sevryugina, Y. V. An Efficient Halogen-Free Electrolyte for Use in Rechargeable Magnesium Batteries. *Angew. Chem., Int. Ed.* **2015**, *54*, 7900−7904.
(16) Keyzer, E. N.; Glass, H. F. J.; Liu, Z.; Bayley, P. M.; Dutton, S. E.; Grey, C. P.; Wright, D. S. $Mg(PF_6)_2$-Based Electrolyte Systems: Understanding Electrolyte−Electrode Interactions for the Development of Mg-Ion Batteries. *J. Am. Chem. Soc.* **2016**, *138*, 8682−8685.
(17) Krossing, I.; Raabe, I. Noncoordinating Anions—Fact or Fiction? A Survey of Likely Candidates. *Angew. Chem., Int. Ed.* **2004**, *43*, 2066−2090.
(18) Bulut, S.; Klose, P.; Huang, M.-M.; Weingärtner, H.; Dyson, P. J.; Laurenczy, G.; Friedrich, C.; Menz, J.; Kümmerer, K.; Krossing, I. Synthesis of Room-Temperature Ionic Liquids with the Weakly Coordinating $[Al(OR^F)_4]^-$ Anion (R^F = C(H) $(CF_3)_2$) and the Determination of Their Principal Physical Properties. *Chem. - Eur. J.* **2010**, *16*, 13139−13154.
(19) Tsujioka, S.; Nolan, B. G.; Takase, H.; Fauber, B. P.; Strauss, S. H. Conductivities and Electrochemical Stabilities of Lithium Salts of Polyfluoroalkoxyaluminate Superweak Anions. *J. Electrochem. Soc.* **2004**, *151*, A1418−A1423.
(20) Buchanan, W. D.; Ruhlandt-Senge, K. M-F Interactions and Heterobimetallics: Furthering the Understanding of Heterobimetallic Stabilization. *Chem. - Eur. J.* **2013**, *19*, 10708−10715.
(21) Krossing, I. The Facile Preparation of Weakly Coordinating Anions: Structure and Characterisation of Silverpolyfluoroalkoxyaluminates $AgAl(OR^F)_4$, Calculation of the Alkoxide Ion Affinity. *Chem. - Eur. J.* **2001**, *7*, 490−502.
(22) Kraft, A.; Trapp, N.; Himmel, D.; Böhrer, H.; Schlüter, P.; Scherer, H.; Krossing, I. Synthesis, Characterization, and Application of Two $Al(OR^F)_3$ Lewis Superacids. *Chem. - Eur. J.* **2012**, *18*, 9371−9380.
(23) Müller, L. O.; Himmel, D.; Stauffer, J.; Steinfeld, G.; Slattery, J.; Santiso-Quiñones, G.; Brecht, V.; Krossing, I. Simple Access to the Non-Oxidizing Lewis Superacid PhF-$Al(OR^F)_3$ (R^F = $C(CF_3)_3$). *Angew. Chem., Int. Ed.* **2008**, *47*, 7659−7663.
(24) Kříž, O.; Čásenský, B.; Lyčka, A.; Fusek, J.; Heřmánek, S. ^{27}Al NMR Behavior of Aluminium Alkoxides. *J. Magn. Reson.* **1984**, *60*, 375−381.
(25) Meese-Marktscheffel, J. A.; Cramer, R. E.; Gilje, J. W. Magnesium-Aluminium Alkoxides: The Synthesis of $Mg[Al(OR)_4]_2$ (R = Bu^{sec} and Ph), Structure of $(thf)_2Mg[(\mu\text{-}OPh)_2Al(OPh)_2]_2$, and Dynamic NMR of $Mg[Al(OBu^{sec})]_4$. *Polyhedron* **1994**, *13*, 1045−1050.
(26) Meese-Marktscheffel, J. A.; Fukuchi, R.; Kido, M.; Tachibana, G.; Jensen, C. M.; Gilje, J. W. Heterometallic Aluminum Alkoxides. The Characterization of $\{Mg[Al(OPr^i)_4]_2\}_n$ and $Mg_2Al_3(OPr^i)_{13}$. *Chem. Mater.* **1993**, *5*, 755−757.
(27) Liu, T.; Shao, Y.; Li, G.; Gu, M.; Hu, J.; Xu, S.; Nie, Z.; Chen, X.; Wang, C.; Liu, J. A Facile Approach Using $MgCl_2$ to Formulate High Performance Mg^{2+} Electrolytes for Rechargeable Mg Batteries. *J. Mater. Chem. A* **2014**, *2*, 3430−3438.
(28) Cheng, Y.; Stolley, R. M.; Han, K. S.; Shao, Y.; Arey, B. W.; Washton, N. M.; Mueller, K. T.; Helm, M. L.; Sprenkle, V. L.; Liu, J.; et al. Highly Active Electrolytes for Rechargeable Mg Batteries Based on a $[Mg_2(\mu\text{-}Cl)_2]^{2+}$ Cation Complex in Dimethoxyethane. *Phys. Chem. Chem. Phys.* **2015**, *17*, 13307−13314.
(29) Takemura, H.; Kon, N.; Kotoku, M.; Nakashima, S.; Otsuka, K.; Yasutake, M.; Shinmyozu, T.; Inazu, T. A Study of C−F···M^+ Interaction: Alkali Metal Complexes of the Fluorine-Containing Cage Compound. *J. Org. Chem.* **2001**, *66*, 2778−2783.
(30) Plenio, H.; Burth, D. ^{19}F NMR Indicator for Protons and Metal Ions with Direct Fluorine−metal Interactions. *J. Chem. Soc., Chem. Commun.* **1994**, *19*, 2297−2298.
(31) Shao, Y.; Liu, T.; Li, G.; Gu, M.; Nie, Z.; Engelhard, M.; Xiao, J.; Lv, D.; Wang, C.; Zhang, J.-G.; et al. Coordination Chemistry in Magnesium Battery Electrolytes: How Ligands Affect Their Performance. *Sci. Rep.* **2013**, *3*, 3130.
(32) Barile, C. J.; Barile, E. C.; Zavadil, K. R.; Nuzzo, R. G.; Gewirth, A. A. Electrolytic Conditioning of a Magnesium Aluminum Chloride Complex for Reversible Magnesium Deposition. *J. Phys. Chem. C* **2014**, *118*, 27623−27630.
(33) Shterenberg, I.; Salama, M.; Yoo, H. D.; Gofer, Y.; Park, J.-B.; Sun, Y.-K.; Aurbach, D. Evaluation of $(CF_3SO_2)_2N^-$ (TFSI) Based Electrolyte Solutions for Mg Batteries. *J. Electrochem. Soc.* **2015**, *162*, A7118−A7128.
(34) Tokuda, H.; Watanabe, M. Characterization and Ionic Transport Properties of Nano-Composite Electrolytes Containing a Lithium Salt of a Superweak Aluminate Anion. *Electrochim. Acta* **2003**, *48*, 2085−2091.
(35) Aurbach, D.; Gofer, Y. The Electrochemical Window of Nonaqueous Electrolyte Solutions. In *Nonaqueous Electrochemistry*; Aurbach, D., Ed.; Marcel Dekker: New York, 1999; pp 137−212.
(36) Markovsky, B.; Amalraj, F.; Gottlieb, H. E.; Gofer, Y.; Martha, S. K.; Aurbach, D. On the Electrochemical Behavior of Aluminum Electrodes in Nonaqueous Electrolyte Solutions of Lithium Salts. *J. Electrochem. Soc.* **2010**, *157*, A423−A429.
(37) Arthur, T. S.; Zhang, R.; Ling, C.; Glans, P.-A.; Fan, X.; Guo, J.; Mizuno, F. Understanding the Electrochemical Mechanism of K-αMnO_2 for Magnesium Battery Cathodes. *ACS Appl. Mater. Interfaces* **2014**, *6*, 7004−7008.
(38) Zhang, R.; Arthur, T. S.; Ling, C.; Mizuno, F. Manganese Dioxides as Rechargeable Magnesium Battery Cathode; Synthetic Approach to Understand Magnesiation Process. *J. Power Sources* **2015**, *282*, 630−638.
(39) Zhang, R.; Yu, X.; Nam, K.-W.; Ling, C.; Arthur, T. S.; Song, W.; Knapp, A. M.; Ehrlich, S. N.; Yang, X.-Q.; Matsui, M. α-MnO_2 as a Cathode Material for Rechargeable Mg Batteries. *Electrochem. Commun.* **2012**, *23*, 110−113.
(40) Klankowski, S. A.; Pandey, G. P.; Malek, G.; Thomas, C. R.; Bernasek, S. L.; Wu, J.; Li, J. Higher-Power Supercapacitor Electrodes Based on Mesoporous Manganese Oxide Coating on Vertically Aligned Carbon Nanofibers. *Nanoscale* **2015**, *7*, 8485−8494.
(41) Lapidus, S. H.; Rajput, N. N.; Qu, X.; Chapman, K. W.; Persson, K. A.; Chupas, P. J. Solvation Structure and Energetics of Electrolytes

DOI: 10.1021/acsenergylett.6b00356
ACS Energy Lett. 2016, 1, 1227−1232

for Multivalent Energy Storage. *Phys. Chem. Chem. Phys.* **2014**, *16*, 21941−21945.

(42) Wan, L. F.; Perdue, B. R.; Apblett, C. A.; Prendergast, D. Mg Desolvation and Intercalation Mechanism at the Mo_6S_8 Chevrel Phase Surface. *Chem. Mater.* **2015**, *27*, 5932−5940.

DOI: 10.1021/acsenergylett.6b00356
ACS Energy Lett. 2016, 1, 1227−1232